

Available online at www.sciencedirect.com

jmr&t
Journal of Materials Research and Technology
journal homepage: www.elsevier.com/locate/jmrt



Original Article

Flexible piezoelectric PVDF/TPU nanofibrous membranes produced by solution blow spinning



Bao Le ^{a,*}, Nada Omran ^b, Ahmed H. Hassanin ^{b,c,d}, Ishac Kandas ^{b,e},
Mohammed Gamal ^b, Nader Shehata ^{b,e,g,h}, Islam Shyha ^{a,f}

^a School of Computing Engineering and the Built Environment, Edinburgh Napier University, Edinburgh, UK

^b Center of Smart Materials Nanotechnology and Photonics (CSMNP), Smart CI Research Center, Alexandria University, Alexandria 21544, Egypt

^c Materials Science & Engineering Department, School of Innovative Design Engineering, Egypt-Japan University of Science and Technology (E-JUST), New Borg El-Arab City, Alexandria 21934, Egypt

^d Department of Textile Engineering, Faculty of Engineering, Alexandria University, Alexandria 21544, Egypt

^e Department of Engineering Mathematics and Physics, Faculty of Engineering, Alexandria University, Alexandria 21544, Egypt

^f Department of Production Engineering, Faculty of Engineering, Alexandria University, Alexandria 21544, Egypt

^g Kuwait College of Science and Technology (KCST), Doha District 13133, Kuwait

^h USTAR Bioinnovations Center, Faculty of Science, Utah State University, Logan, UT 84341, USA

ARTICLE INFO

Article history:

Received 3 August 2022

Accepted 6 April 2023

Available online 14 April 2023

Keywords:

Piezoelectric

PVDF

TPU

Solution blow spinning

Nanofibers

Elasticity

Energy harvesting

ABSTRACT

Poly (vinylidene fluoride) (PVDF) nanofibers have been applied in producing piezoelectric membranes for energy harvesting in wearable devices under strenuous service conditions due to its outstanding properties such as piezoelectricity, flexibility, stability, and biocompatibility. Therefore, a processing technique with mass production capability and generating the highest possible piezoelectric properties of PVDF nanofibers is required. To achieve such requirements, this study presented a novel flexible piezoelectric membrane based on PVDF/TPU nanofibers using solution blow spinning (SBS). The addition of TPU into PVDF has been proven to increase the flexibility of the polymeric membranes. The produced membranes showed high piezoelectric response and sensitivity compared to other PVDF-based membranes in the literature especially at 5wt.% TPU concentration, owing to its small nanofiber diameter, high β fraction, and inducing reorientation of electric dipoles. The addition of TPU also significantly enhanced tensile strength and elasticity of the produced membranes. Based on those, this work has shown a promising method to produce high elastic-piezoelectric nanofibrous membrane using SBS.

© 2023 The Authors. Published by Elsevier B.V. This is an open access article under the CC BY license (<http://creativecommons.org/licenses/by/4.0/>).

* Corresponding author.

E-mail address: B.Le@napier.ac.uk (B. Le).

<https://doi.org/10.1016/j.jmrt.2023.04.051>

2238-7854/© 2023 The Authors. Published by Elsevier B.V. This is an open access article under the CC BY license (<http://creativecommons.org/licenses/by/4.0/>).

1. Introduction

Since discovered in 1880 [1], piezoelectric materials (PEMs) have been researched and applied in electronics such as sensors, piezoelectric motors, and mobile phones [2–4]. However, energy harvesting is one of the most promising applications of PEMs. Energy harvesting is process of collecting energy from different sources such as heat, mechanical vibrations and deformations and converting into electrical energy [5]. In recent decades, the advanced technologies in semiconductor production have prompted remarkable progressions in miniaturizing electronic devices, including portable electronics, transmitters, and sensors, hence improving their functionality and energy efficiency [6]. In the context of mechanical vibrations and deformations, there are different approaches to transfer these mechanical energies into electrical energy including electromagnetic [7], electrostatic [8] and piezoelectric effects [9]. Among these, piezoelectric effect is preferable due to its high flexibility, simple configuration, high conversion efficiency [10]. Subsequently, PEMs have been used in producing integrated microelectromechanical systems (MEMS) that have been applied in automotive industry, smartphones, and other everyday applications as energy harvesters [11]. There are various PEMs that have been studied in the past decades. Piezo ceramics such as lead zirconate titanate (PZT) and barium titanate (BaTiO_3) attracted more research attention due to their high piezoelectric coefficient, good performance in energy harvesting compared to other PEMs [12]. For example, the piezoelectric coefficient of PZT is 175 pC/N with high electromechanical coupling coefficient, mechanical quality factor and elastic stiffness [13]. Therefore, PZT and BaTiO_3 thin films have been extensively studied in energy harvesting applications [14]. However, these piezo ceramics also possess some serious drawbacks including toxicity, high brittleness, rigidity, low voltage coefficient, limited design flexibility and complex fabricating procedure, hence limiting their usage in energy harvesting applications [15]. Therefore, it is necessary to find alternative piezoelectric materials that exhibit high flexibility while still maintaining high piezoelectric performance and stability. These requirements are crucial for PEMs to be applied in flexible electronics such as wearable devices. The discovery of piezoelectric polymers provided high potential to overcome inherent drawbacks of piezoelectric ceramic materials due to their high flexibility, biocompatibility, simple processing, and fabrication. Various piezoelectric polymers have been studied in the field of energy harvesting including PVDF, polyurethanes (PU), polyimides (PI), polylactic acid (PLA) [16]. Among these, PVDF exhibits high piezoelectric coefficient, reasonable mechanical strength, elasticity, biocompatibility, and chemical resistance [17–20].

Solution blow spinning (SBS) has been applied as an alternative technique of electrospinning in producing sub-micron/nanofibers. Unlike electrospinning, SBS can be used for both electrically conductive and nonconductive systems as no electrical field is required to operate fiber extrusion process. Also, this technique possesses high production yield and simple setup, resulting in high possibility to be scaled up [21].

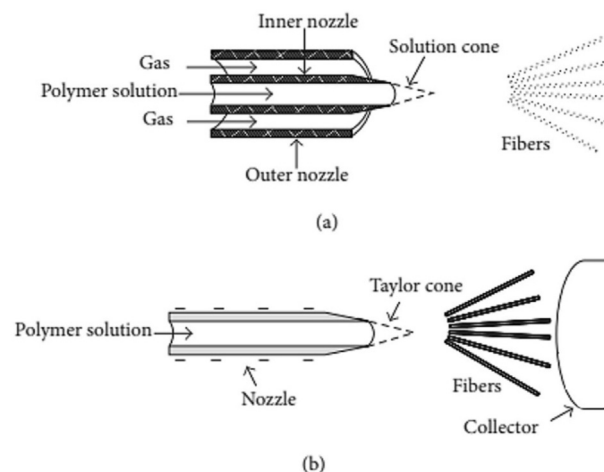


Fig. 1 – The schematic representing the working principle of: (a) Solution blow spinning, and (b) Electrospinning [23].

This technique employs a concentric nozzle containing two coaxial channels with a polymer solution injected through inner channel into a pressurized air flow from the surrounding outer channel. The solution droplet formed at the nozzle tip is then stretched by the compressed air around and its surface is distorted into a solution cone like Taylor cone in electrospinning to generate fine liquid jets. As the solution jets travel across the working distance, the solvent evaporates, leaving the polymer fibers on the surface of the collector [22]. (see Fig. 1).

In this paper, the fabrication of PVDF/TPU nanofibrous membrane using SBS was presented. The aim of this work was to investigate the piezo-elastic properties of the membranes considering the effect of TPU addition at different contents. Solution blow spun nanofibers were characterized by scanning electron microscopy (SEM), Fourier-transform infrared spectroscopy (FTIR). Their piezoelectric and mechanical properties were indicated by cyclic load and tensile tests, respectively.

2. Experimental

2.1. Materials

Poly (vinylidene fluoride) (PVDF) (Kynar® 761, King of Prussia, PA, USA) was supplied by ARKEMA and thermoplastic polyurethane (TPU) with Polydispersity Index (PDI) of 1.83 and molecular weight of 107,020 g mol⁻¹ was supplied by (BASF Co., Ltd., Berlin, Germany). Known polymer concentrations were dispersed in dimethylformamide (DMF 98%, Sigma Aldrich, Taufkirchen, Germany).

2.2. Solution preparation and characterization

A fixed concentration of 15% polymer blend of different PVDF-TPU ratios was dispersed in DMF solvent. The solutions were magnetic stirred for 24 h at room temperature before the SBS

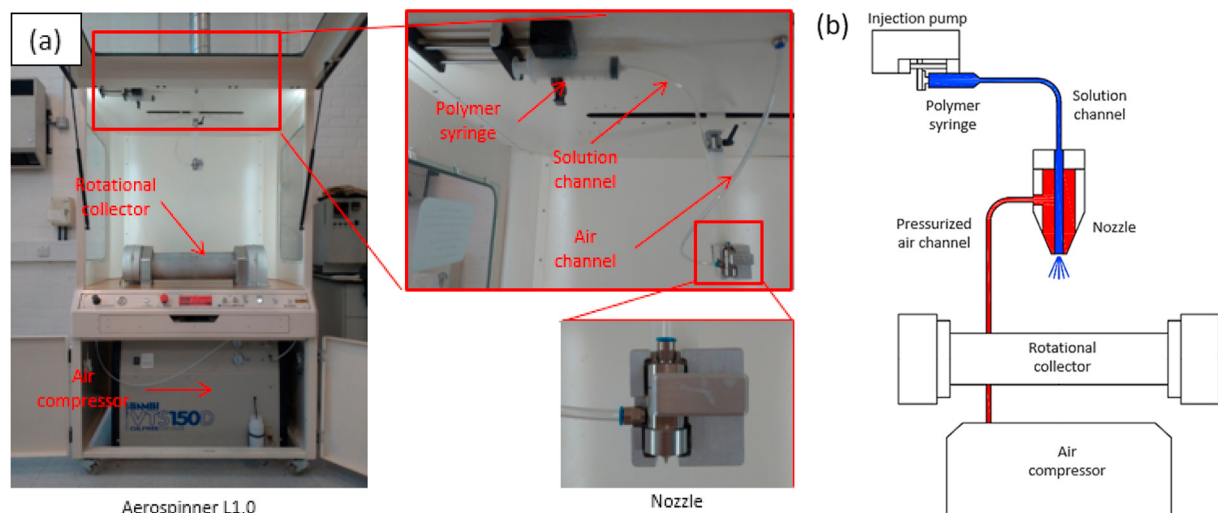


Fig. 2 – Solution blow spinning: (a) Processing setup, and (b) schematic.

process to obtain homogenous blend. Four different TPU concentrations were used in this study including 5, 10, 15, and 20wt.%. The neat PVDF was also employed as a benchmark. The viscosity of the solutions was determined using a rotary viscometer (DV-II+, Brookfield, USA) at room temperature.

2.3. Solution blow spinning

Lab scale solution blowing device Areka Aerospinner L1.0 was used to perform SBS process in this study. A plastic syringe filled with the polymer solution was connected to the solution blow spinning custom-made concentric nozzle (AREKA group, Turkey). The solution was pumped with a syringe pump SN-50C6 (Sino Medical-Device Technology Co., Ltd, Shenzhen, China) through a needle of 18 gauge at a feed rate of 10 mL/h. Air pressure supplied by Bambi VTS150D air compressor was fixed at 4 bar for all processing conditions. A rotational

collector with a mesh length of 22 cm and outer diameter of 14 cm was used to collect the blow spun nanofibers. The distance between the nozzle and the rotating collector was approximately 45 cm. The experiment setup and its schematic are shown in Fig. 2.

2.4. Morphological and physical characterization

The morphology of the solution blow spun PVDF/TPU nanofibers was characterized using scanning electron microscopy (SEM) (Tescan, Vega3). The samples were coated with platinum to achieve high-quality SEM images. Quantitative analyses of the average fiber diameters and their distributions were also conducted using measuring tool of the SEM by taking 50 measurements from 3 SEM photos for each sample. A Fourier transform infrared spectrometer (FT-IR) (PerkinElmer Frontier) was operated in ATR mode to calculate the β

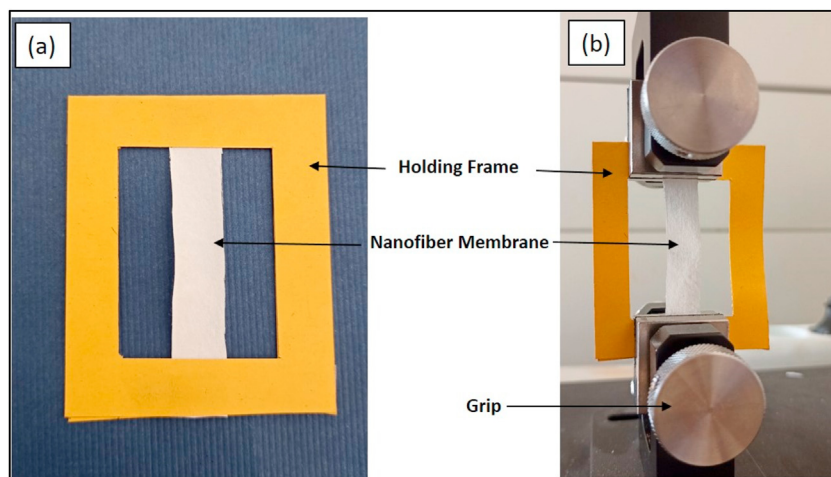


Fig. 3 – Tensile test: (a) Sample with holding frame, and (b) Setup.

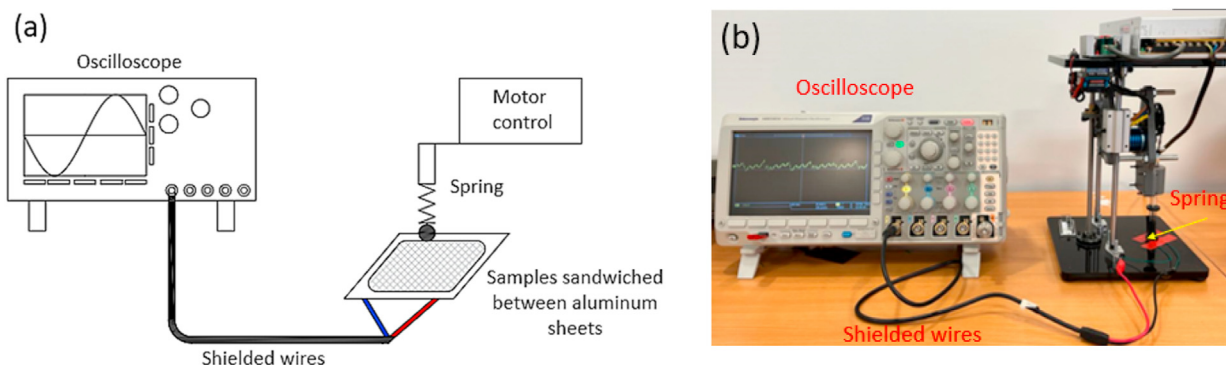


Fig. 4 – Piezoelectric characterization: (a) Schematic, and (b) Setup.

phase content of PVDF/TPU nanofibers. Samples were scanned 120 times at a resolution of 5 cm^{-1} over a range of $4000\text{--}400\text{ cm}^{-1}$.

2.5. Mechanical characterization

Tensile tests were performed on PVDF/TPU nanofibrous membranes to characterize tensile properties of the produced samples considering the effect of different TPU concentrations. The samples were cut into rectangular strips with dimensions of $10 \times 40\text{ mm}$. These samples were integrated into a cardboard holding frame. The nanofibrous membranes were tested with 3 samples from the same setting to calculate the average value. A universal mechanical testing machine (Texture Analyzer CTX, AMETEK Brookfield) was employed to conduct the tensile tests with 10 mm min^{-1} strain rate, zero initial load, 100 N load cell at room temperature. The setup of tensile test is shown in Fig. 3.

2.6. Piezoelectric characterization

The piezoelectric characterization of the solution blown PVDF/TPU nanofibrous membranes was performed on a custom-made set up Fig. 4 consisting of a DC motorized spring having an electronic speed controller. To study the piezoelectric property, a sample of dimensions $1.5\text{ cm} \times 1.5\text{ cm}$ and $0.02\text{--}0.03\text{ mm}$ thickness was first sandwiched between two sheets of aluminum foil as electrodes and shielded copper wires are attached from both sides of these two electrodes. The other ends of the shielded wires were connected to high impedance mixed domain oscilloscope (Tektronix MDO3012) to detect and display the generated piezoelectric voltage in the direction of the thickness d_{33} . According to theory, the d_{33} represents the ratio of the electric charge q that is produced in response to an applied force F as shown in Equation (1):

$$d_{33} = \frac{dq}{dF} \quad (1)$$

Where dF denotes the differential change in applied force along the thickness of the piezoelectric nanofiber, and dq denotes the differential change in charge. The d_{33} coefficient is determined by applying 250 mN with 110 Hz to the sample using the (YE2730, APC, USA). Wide-range d_{33} Meter by constructing

a sample with $0.25\text{--}0.3\text{ mm}$ thickness from several layers with the same direction of polarization. Some materials parameters can be calculated through the following equations:

$$\epsilon_{r33} = \frac{C_{33}t}{\epsilon_0 A} \quad (2)$$

$$V_{33} = \frac{d_{33}t}{\epsilon_0 \epsilon_r A} F \quad (3)$$

$$g_{33} = \frac{d_{33}}{\epsilon_0 \epsilon_r} \quad (4)$$

where t is thickness, A is the area, V is the output voltage, C capacitance, g is the voltage constant, and F is the applied force.

The cyclic forces or loads with 1 cm diameter at different frequencies were applied on to the sample thereby resulting in piezoelectric response of these material compositions in nanoscale indicated by the output voltages. The applied force on to the sample was varied by adjusting the compression length of the spring using a standard calibration tool. The peak-to-peak voltage generated in response to each cyclic force in the range of few newtons was recorded using the oscilloscope. The force was applied at different frequencies from 0.5 to 2 Hz by using the speed controller of the motor that drives the spring vertically.

3. Results and discussion

3.1. Viscosity

Due to the important role of viscosity of polymer solution in affecting the morphology and diameter of produced fibers, it is

Table 1 – Viscosity of PVDF/TPU solutions.

TPU content (wt.%)	Viscosity (cps)
0	810
5	780
10	950
15	1000
20	1200

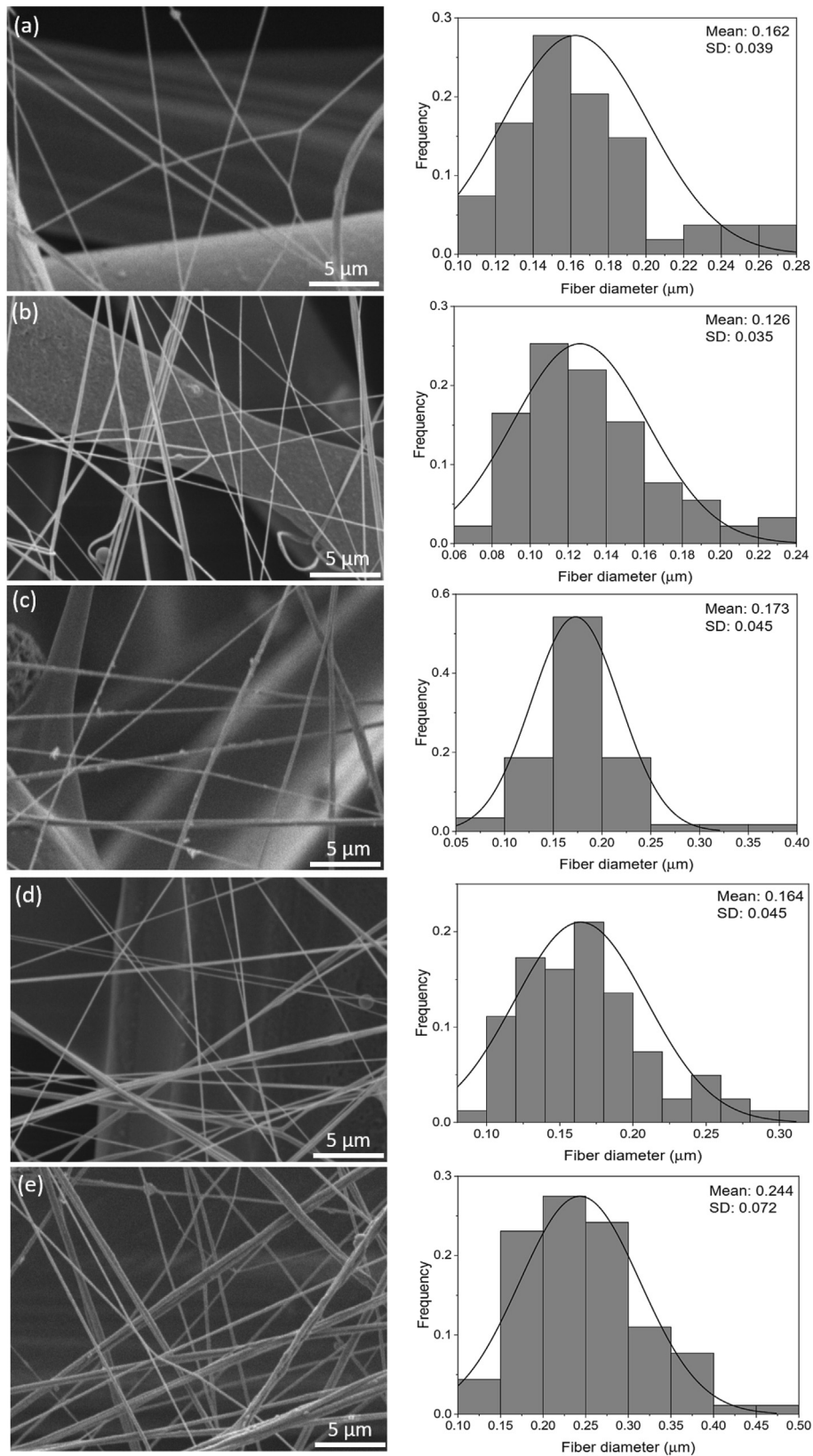


Fig. 5 – PVDF/TPU nanofiber morphology with diameter distribution. (a) PVDF, (b) 5wt.% TPU, (c) 10wt.% TPU, (d) 15wt.% TPU, and (e) 20wt.% TPU.

necessary to be identified. Table 1 shows the viscosity of 15% PVDF/TPU solutions at different TPU contents. It was seen that the viscosity of these solutions was generally increased with more TPU added. It was due to the high molecular weight of TPU that contributed to high degree of molecular chain entanglement of the PVDF/TPU blend. This showed high agreement with the literature when PVDF/TPU blends with less than 25wt.% TPU were considered [24]. TPU as a plasticizer could increase miscibility of the PVDF solution via forming hydrogen bonds, hence elevating viscosity [25]. However, the viscosity at 5wt.% TPU was slightly lower than that of PVDF solution. This deviate phenomenon was possibly due to interfacial slip between in-compatible phases that contributed by weak interaction between PVDF and TPU at such low content of TPU [26].

3.2. Morphological analysis

Fig. 5 shows the SEM images of PVDF/TPU nanofibers at different concentrations of TPU (from 0 to 20wt.%) with their corresponding histograms of fiber diameter distribution. The results show the fiber diameter in the range from 100 to 500 nm. The addition of TPU showed no negative impact on fiber morphology as bead-free fibers and relatively normal distribution of fiber diameter were observed from SEM images at all TPU fractions. It was a result of homogenous polymer blend solution as well as optimized SBS conditions and polymer concentration. However, the effect of TPU concentration on increasing nanofiber diameter was relatively obvious as can be seen from Table 2. Fiber diameter generally increased with more TPU added with an exceptional reduction can be seen at 5wt.% TPU. This variation trend of fiber diameter is consistent with its corresponding solution viscosity shown in Table 1 that indicated the obvious effect of high viscosity of polymer solution on increasing fiber diameter [27]. It was due to large surface tension of polymer solution at high viscosity weakened attenuation force from pressurized air, resulting in large fiber produced compared to those at low viscosity. Based on this analysis, it can be seen that the solution viscosity contributed to the decrease of fiber diameter at 5wt.% TPU as well as its increase at higher TPU concentration compared to PVDF nanofibers.

3.3. Crystalline phase analysis

The FT-IR spectra results for PVDF/TPU nanofibrous membrane at different TPU concentrations are shown in Fig. 6. The

Table 2 – Average diameters of PVDF/TPU nanofibers at different TPU contents.				
TPU content (wt.%)	Fiber average diameter (μm)			Standard deviation
	Mean	Median	Mode	
0	0.16	0.15	0.15	0.038
5	0.13	0.12	0.11	0.035
10	0.17	0.17	0.16	0.045
15	0.16	0.16	0.15	0.045
20	0.24	0.23	0.22	0.072

Table 3 – Mechanical Properties of PVDF/TPU nanofibrous membrane at different TPU concentration.

	Strain (%)	Stress (MPa)	Toughness (MPa)
PVDF	4.6 ± 0.4	9.5 ± 0.7	25.76121
5wt.% TPU	5.4 ± 0.5	31.2 ± 2	107.7924
10wt.% TPU	6.2 ± 0.9	32.9 ± 1.9	109.0367
15wt.% TPU	6.7 ± 0.5	33.2 ± 2.7	136.8509
20wt.% TPU	7.9 ± 1	43.9 ± 2.5	224.6001

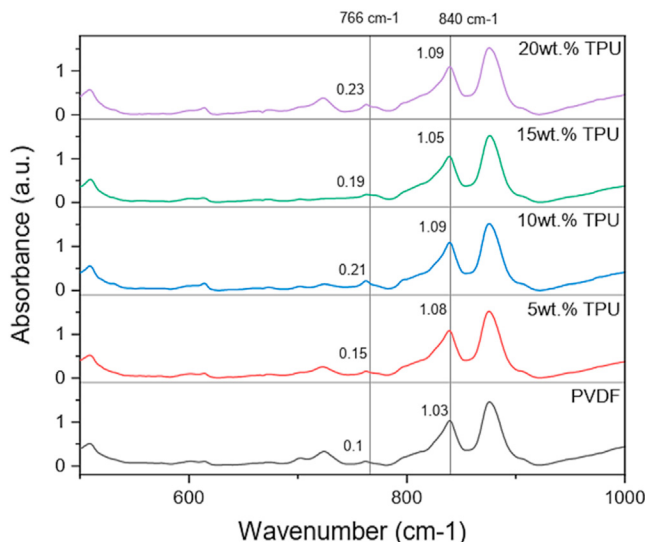


Fig. 6 – FT-IR spectra for PVDF/TPU nanofibrous membrane at different TPU concentrations.

introduction of FT-IR data provides quantitative identification and quantitative analysis of the crystalline phases of PVDF and PVDF/TPU nanofibers including α , β , γ , δ , and ϵ . As piezoelectric properties were concerned in this study, the intensity of the characteristic absorption peaks of the β phase at 840 cm^{-1} relative to those of α phase at 766 cm^{-1} was indicated. This intensity decreased along with increasing TPU

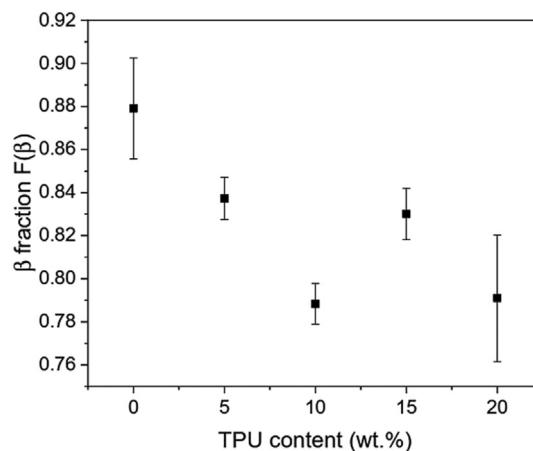


Fig. 7 – Fraction of β phase as a function of TPU content.

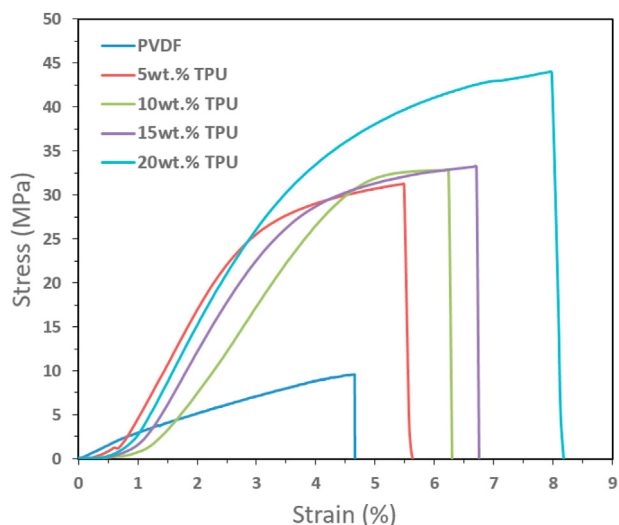


Fig. 8 – Stress–strain curve of PVDF/TPU nanofibrous membrane at different TPU concentration.

concentration compared to PVDF nanofibers. To further quantify this analysis, the fraction of β phase for each composition was calculated using equation derived from Beer–Lambert law:

$$F(\beta) = \frac{A_{\beta}}{1.26 A_{\alpha} + A_{\beta}} \quad (5)$$

where A_{α} and A_{β} are the intensities of absorbance bands at 766 cm^{-1} and 840 cm^{-1} , respectively. The β fraction results are shown in Fig. 7. The β fraction of PVDF nanofibers produced by SBS process in this study was 0.88 which is higher than those of electrospun counterpart (around 0.75) [28]. On the other hands, the general reduction of β phase can be observed for all

compositions. However, this reduction was only significant at 10wt.% and 20wt.% TPU concentrations (around 0.79) while it still maintained a relatively high β phase fraction at 5wt.% TPU (0.84) following by 15wt.% composition (0.83) compared to that of PVDF. These results can be qualitatively explained based on fiber diameter. In SBS process, thinner fibers result from higher level of bending and stretching, leading to more transformation from α to β phase. The fibers from 10wt.% and 20wt.% TPU compositions showed higher diameters compared to the others (Table 2), hence exhibiting lower β fractions. Using 5wt.% [25] and 15wt.% TPU [29] have been indicated to improve the β fraction of electrospun PVDF nanofibers due to the impact of TPU mechanical elasticity on enhancing dipole reorientation.

3.4. Mechanical analysis

Tensile test was conducted for all samples at different compositions to investigate the effect of adding TPU on mechanical properties of PVDF nanofibers (Table 3). Their stress–strain curves are shown in (Fig. 8). It was obvious that the addition of TPU significantly enhance the mechanical properties of the produced membranes. The PVDF/TPU nanofibrous membranes showed significantly higher tensile strength, regardless the TPU concentration. Tensile strength was around 3.5 times higher than PVDF counterpart for 5, 10, and 15wt.% TPU while 20wt.% TPU composition exhibited maximum value at ($\sim 44 \pm 2.5$) MPa. The flexibility of the nanofibrous membranes showed a similar trend with tensile strength due to TPU addition, exhibiting by the highest failure strain of 20wt.% TPU (7.9 ± 2 %), following by other PVDF/TPU compositions ($\sim 6 \pm 1$ %) compared to PVDF (4.6 ± 0.4 %). The addition of TPU as a ductile elastomer contributed to elongation improvement in PVDF/TPU blends. Furthermore, the enhancements of both tensile strength and elongation in this case indicated the high compatibility of PVDF/TPU blends. These mechanical

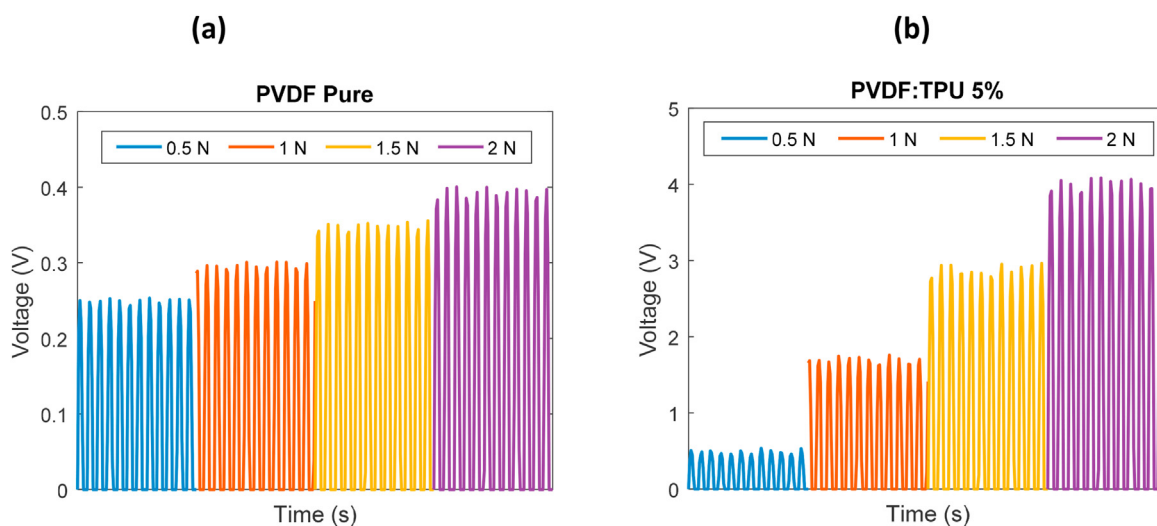


Fig. 9 – Examples to the output generated voltage under different applied forces at 0.5 Hz for a) pure PVDF nanofibers, and b) PVDF:TPU 95:5 %.

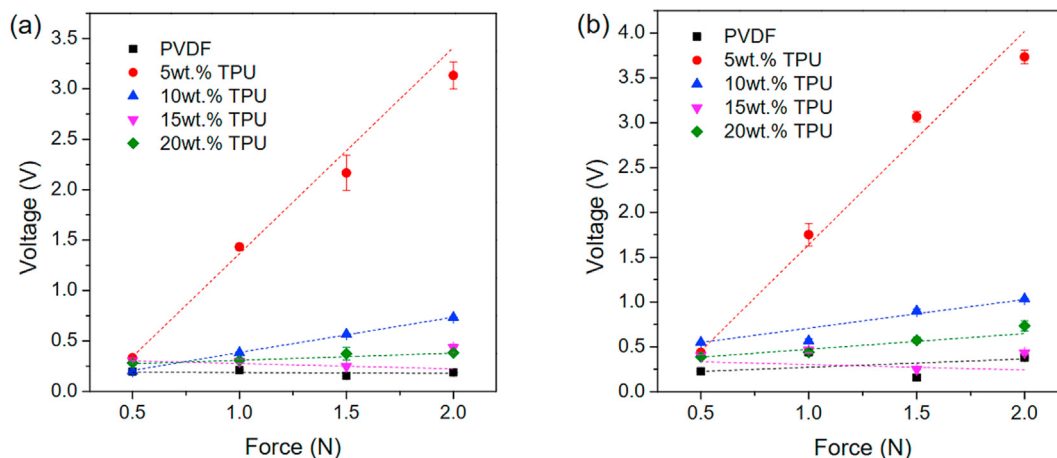


Fig. 10 – Piezoelectric response of PVDF/TPU nanofibrous membranes at different TPU concentrations as a function of applied force at frequency of: (a) 0.5 Hz, and (b) 2 Hz.

enhancements can provide PVDF/TPU nanofibrous membrane a large range of applications that need piezoelectric materials with high elasticity under high-frequency load such as air filtration [30] and footstep generation in energy harvesting [31].

3.5. Piezoelectric analysis

The piezoelectric responses displayed by output voltage for all PVDF/TPU blends under different magnitudes of applied force are shown in Fig. 9. Generally, the addition of TPU enhanced the piezoelectric response in the direction of the applied force d_{33} of produced nanofibrous membranes compared to that of PVDF counterpart. Among all PVDF/TPU compositions, 5wt.% TPU exhibited the most improved piezoelectric response, indicated by a nearly linear increase of its resulting voltage along with increasing applied force. However, a further increase of TPU concentration over 5% degraded the piezoelectric response, exhibited by the drop of generated voltage at higher TPU concentrations. The effect of TPU addition on improving the piezoelectric response of PVDF in this work, especially at 5wt.% TPU showed high agreement with a recent study investigated the piezoelectric coefficient of PVDF blended with TPU and bismuthsodium titanate polycrystalline oxide (BNT) [25]. This study indicated a significant enhancement of face shear piezoelectric coefficient (d_{36}) at a small TPU content added (≤ 5 wt.%), a nearly linear increase of d_{36} in the range of 5–20wt.% and then decreased over 20wt.% [25]. Now, an example of recent study of enhancing the piezoelectric response in the direction of applied force when the TPU is added to the PVDF with concentration of 15% [29]. In our work, we calculated the d_{33} for all PVDF:TPU blended concentration and we found that the 5wt.% TPU is the best piezoelectric coefficient. Both Figs. S1 and S2 show the piezo force microscope of PVDF and PVDF:TPU nanofibers membranes to give an extra proof to the enhancement of piezoelectric response through increased surface roughness under applied electric potential. Fig. 9 shows examples to the generated voltage under different applied forces for some of the PVDF:TPU solution-blown spun nanofibers samples.

Fig. 10 shows the relation between the applied force and corresponding generated voltage at different vibrational frequencies for all targeted samples. Thus, the addition of 5wt.% TPU improved the piezoelectric response of the membrane, as shown in Fig. 10. It consequently resulted in enhanced output voltage at the same applied force. The reduction of β phase fraction as further TPU content added (over 5%) should be more dominant mechanism in decreasing the piezoelectric response of others PVDF/TPU compositions (10–20wt.%). The significant improvement of piezoelectric response of nanofibrous membranes at 5wt.% TPU led to its highest piezoresponse sensitivity regardless the applied frequency that can be seen from Fig. 11. The piezoresponse sensitivity of 5wt.% TPU composition can reach to its maximum value of 1.8 V/N at 2 Hz. This magnitude of piezoresponse sensitivity is much higher than other PVDF-based piezoresponse membranes in literature [32,33].

Also, different parametric analysis of the targeted samples has been shown in Table 4, which shows the enhancement of both piezoelectric coefficient and dielectric constant due to the added TPU with 5 wt.%. Also, we have shown the

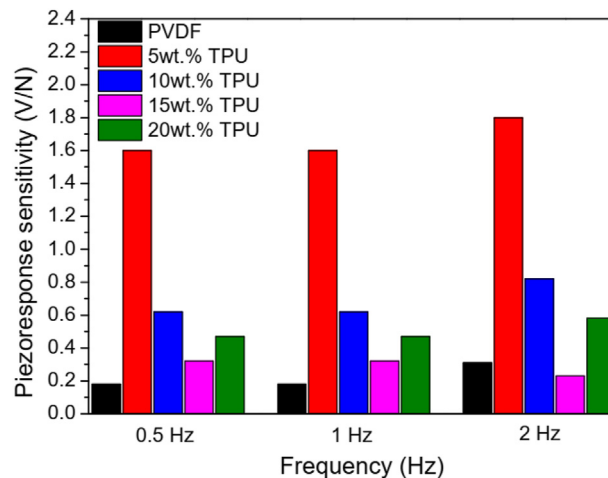


Fig. 11 – Piezoresponse sensitivity of PVDF/TPU nanofibrous membranes at different TPU concentrations.

Table 4 – Materials parameters and both expected and measured voltages from different PVDF:TPU samples.

	TPU 0%	TPU 5%	TPU 10%	TPU 15%	TPU 20%
C_{33} (PF)	28.1	30.4	42.7	33.7	19.8
t (mm)	0.05	0.097	0.037	0.06	0.09
d_{33} (PC/N)	45.5	154.58	65.15	48.5	35.2
ϵ_r	2.47	5.18	2.057	2.97	3.494
g_{33} (Vm/N)	2.081	3.370	3.577	1.844	1.138
V_{th} (V)	1.625	5.092	2.085	1.729	1.600
V_{exp} (V)	0.35	1.75	0.7	0.4	0.5

theoretical expected voltage in case of thin film of the studied composites, which show that the added 5 wt.% of TPU can lead to the best generated voltage. This trend is the same within the experimental generated voltage, but the numbers are less due to the nanofibers mature of the membrane with porous parts which can reduce the counts of the dipoles which can be exposed to the applied force.

4. Conclusions

In this study, a novel piezoelectric membrane made from PVDF/TPU nanofibers using SBS process. The membranes showed high piezoelectric response and sensitivity under various applied forces with their highest values of 3.7 V and 1.8 N.V⁻¹ under applied force of 2 N and frequency of 2 Hz, respectively. These values are higher than those of other PVDF-based piezoresponse membranes in literature. It was due to high miscibility of the polymer blend (at ≤ 20 wt.% TPU) and optimal processing conditions of SBS that resulted in small nanofiber diameters with normal distribution and their defect-free morphology. It consequently led to higher β fraction of PVDF/TPU nanofibers compared to other PVDF-based membranes produced by electrospinning. The optimum TPU content was found at 5wt.% since it exhibited the best piezoelectric characteristic based on their highest values of both piezoelectric response and sensitivity compared to the others. This conclusion was confirmed by various measurements of output voltage generated under different amplitudes and frequencies of applied forces. Based on that, it can be concluded that SBS is a suitable method to produce piezoelectric nanofibrous membrane due to its high performance in terms of generating high piezoelectric properties. It was also noticed that this innovative elastic-piezo nanofibrous membrane showed high potential to be applied in energy harvesting devices and wearable electronics.

Funding

British Council (352360451).

Declaration of Competing Interest

The authors declare the following financial interests/personal relationships which may be considered as potential competing interests: Bao Le reports financial support was

provided by Newton Fund. Islam Shyha reports a relationship with Newton Fund that includes: funding grants.

Appendix A. Supplementary data

Supplementary data to this article can be found online at <https://doi.org/10.1016/j.jmrt.2023.04.051>.

REFERENCES

- [1] Ikeda T. *Fundamentals of piezoelectricity*. Oxford University Press; 1990.
- [2] Emamian S, Narakathu BB, Chlaihawi AA, Bazuin BJ, Atashbar MZ. Screen printing of flexible piezoelectric based device on polyethylene terephthalate (PET) and paper for touch and force sensing applications. *Sensor Actuator Phys* 2017;263:639–47.
- [3] Lee HS, Chung J, Hwang G, Jeong CK, Jung Y, Kwak J, et al. Flexible inorganic piezoelectric acoustic nanosensors for biomimetic artificial hair cells. *Adv Funct Mater* 2014;24(44):6914–21.
- [4] Persano L, Dagdeviren C, Su Y, Zhang Y, Girardo S, Pisignano D, et al. High performance piezoelectric devices based on aligned arrays of nanofibers of poly (vinylidene fluoride-co-trifluoroethylene). *Nat Commun* 2013;4(1):1–10.
- [5] Kang M-G, Jung W-S, Kang C-Y, Yoon S-J. Recent progress on PZT based piezoelectric energy harvesting technologies. *Actuators* 2016;5(1):5. MDPI.
- [6] Li H, Tian C, Deng ZD. Energy harvesting from low frequency applications using piezoelectric materials. *Appl Phys Rev* 2014;1(4):041301.
- [7] Edwards B, Hu PA, Aw KC. Validation of a hybrid electromagnetic–piezoelectric vibration energy harvester. *Smart Mater Struct* 2016;25(5):055019.
- [8] Naito Y, Uenishi K. Electrostatic MEMS vibration energy harvesters inside of tire treads. *Sensors* 2019;19(4):890.
- [9] Dagdeviren C, Joe P, Tuzman OL, Park K, Lee KJ, Shi Y, et al. Recent progress in flexible and stretchable piezoelectric devices for mechanical energy harvesting, sensing and actuation. *Extreme mechanics letters* 2016;9:269–81.
- [10] Yang Z, Erturk A, Zu J. On the efficiency of piezoelectric energy harvesters. *Extreme Mechanics Letters* 2017;15:26–37.
- [11] Toshiyoshi H, Ju S, Honma H, Ji C-H, Fujita H. MEMS vibrational energy harvesters. *Sci Technol Adv Mater* 2019;20(1):124–43.
- [12] Yang Z, Zhou S, Zu J, Inman D. High-performance piezoelectric energy harvesters and their applications. *Joule* 2018;2(4):642–97.
- [13] Sappati KK, Bhadra S. Piezoelectric polymer and paper substrates: a review. *Sensors* 2018;18(11):3605.
- [14] Safaei M, Sodano HA, Anton SR. A review of energy harvesting using piezoelectric materials: state-of-the-art a decade later (2008–2018). *Smart Mater Struct* 2019;28(11):113001.
- [15] Ramadan KS, Sameoto D, Evoy S. A review of piezoelectric polymers as functional materials for electromechanical transducers. *Smart Mater Struct* 2014;23(3):033001.
- [16] Mishra S, Unnikrishnan L, Nayak SK, Mohanty S. Advances in piezoelectric polymer composites for energy harvesting applications: a systematic review. *Macromol Mater Eng* 2019;304(1):1800463.

- [17] Nguyen VS, Badie L, Sénéchault E, Blampain E, Vincent B, Venet C, et al. Flexible over-moded resonators based on P (VDF-TrFE) thin films with very high temperature coefficient. *IEEE Trans Ultrason Ferroelectrics Freq Control* 2013;60(10):2039–43.
- [18] Nguyen VS, Badie L, Lamouroux E, Vincent B, Santos FDD, Aufray M, et al. Nanocomposite piezoelectric films of P (VDF-TrFE)/LiNbO₃. *J Appl Polym Sci* 2013;129(1):391–6.
- [19] Mayeen A, Kala MS, Jayalakshmy MS, Thomas S, Rouxel D, Phillip J, et al. Dopamine functionalization of BaTiO₃: an effective strategy for the enhancement of electrical, magnetoelectric and thermal properties of BaTiO₃-PVDF-TrFE nanocomposites. *Dalton Trans* 2018;47(6):2039–51.
- [20] Hadji R, Vincent B, Rouxel D, Bauer F. Preparation and characterization of P (VDF-TrFE)/Al₂O₃ nanocomposite. *IEEE Trans Ultrason Ferroelectrics Freq Control* 2012;59(1):163–7.
- [21] Wojasiński M, Pilarek M, Ciach T. Comparative studies of electrospinning and solution blow spinning processes for the production of nanofibrous poly (L-lactic acid) materials for biomedical engineering. *Pol J Chem Technol* 2014;16(2).
- [22] Oliveira JE, Moraes EA, Costa RGF, Afonso AS, Mattoso LHC, Orts WJ, et al. Nano and submicrometric fibers of poly (D, L-lactide) obtained by solution blow spinning: process and solution variables. *J Appl Polym Sci* 2011;122(5):3396–405.
- [23] Oliveira JE, Mattoso LH, Orts WJ, Medeiros ES. Structural and morphological characterization of micro and nanofibers produced by electrospinning and solution blow spinning: a comparative study. *Adv Mater Sci Eng* 2013:2013.
- [24] Cheng J, Wang S, Chen S, Zhang J, Wang X. Properties and crystallization behavior of poly (vinylidene fluoride)(PVDF)/thermoplastic polyurethane elastomer (TPU) blends. *Desalination Water Treat* 2011;34(1–3):184–9.
- [25] Dai Z, Feng Z, Feng C, Meng L, Li C, Wang C, et al. Thermoplastic polyurethane elastomer induced shear piezoelectric coefficient enhancement in bismuth sodium titanate–PVDF composite films. *J Appl Polym Sci* 2021;138(6):49818.
- [26] Ma H, Yang Y. Rheology, morphology and mechanical properties of compatibilized poly (vinylidene fluoride)(PVDF)/thermoplastic polyurethane (TPU) blends. *Polym Test* 2008;27(4):441–6.
- [27] Andrew J, Mack J, Clarke D. Electrospinning of polyvinylidene difluoride-based nanocomposite fibers. *J Mater Res* 2008;23(1):105–14.
- [28] He Z, Rault F, Lewandowski M, Mohsenzadeh E, Salaün F. Electrospun PVDF nanofibers for piezoelectric applications: a review of the influence of electrospinning parameters on the β phase and crystallinity enhancement. *Polymers* 2021;13(2):174.
- [29] Shehata N, Nair R, Boualayan R, Kandas I, Masrani A, Elnabawy E, et al. Stretchable nanofibers of polyvinylidene fluoride (PVDF)/thermoplastic polyurethane (TPU) nanocomposite to support piezoelectric response via mechanical elasticity. *Sci Rep* 2022 May 18;12:8335. <https://doi.org/10.1038/s41598-022-11465-5>.
- [30] Wang L-Y, Liya EY, Lai J-Y, Chung T-S. Developing ultra-high gas permeance PVDF hollow fibers for air filtration applications. *Sep Purif Technol* 2018;205:184–95.
- [31] Nia EM, Zawawi NAWA, Singh BSM. A review of walking energy harvesting using piezoelectric materials. *IOP Conf Ser Mater Sci Eng* 2017;291(1):012026. IOP Publishing.
- [32] Elnabawy E, Hassanain AH, Shehata N, Popelka A, Nair R, Yousef S, et al. Piezoelastic PVDF/TPU nanofibrous composite membrane: fabrication and characterization. *Polymers* 2019;11(10):1634.
- [33] Wu C-M, Chou M-H, Zeng W-Y. Piezoelectric response of aligned electrospun polyvinylidene fluoride/carbon nanotube nanofibrous membranes. *Nanomaterials* 2018;8(6):420.